Biogeosciences
Discussions

Characterising the surface microlayer in the Mediterranean Sea: trace metals concentration and microbial plankton abundance

Antonio Tovar-Sánchez[1], Araceli Rodríguez-Romero[1], Anja Engel[2], Birthe Zäncker[2], Franck Fu[3], Emilio Marañón[4], María Pérez-Lorenzo[4], Matthieu Bressac[5,6], Thibaut Wagener[7], Karine Desboeuf[3], Sylvain Triquet[3], Guillaume Siour[3], Cécile Guieu[7]

[1]Department of Ecology and Coastal Management, Institute of Marine Sciences of Andalusia (ICMAN-CSIC), Puerto Real, 07190, Spain
[2]Leibniz Institute of Marine Sciences (IFM-GEOMAR), Kiel, Germany
[3]Laboratoire Interuniversitaire des Systèmes Atmosphériques (LISA), CNRS UMR 7583, Université de Paris, Université Paris-Est-Créteil, Institut Pierre Simon Laplace (IPSL), Créteil, 94000, France
[4]Departamento de Ecología y Biología Animal, Universidad de Vigo, 36310 Vigo, Spain
[5]Institute for Marine and Antarctic Studies, University of Tasmania, Hobart, Tasmania, Australia
[6]Sorbonne Université, CNRS, Laboratoire d'Océanographie de Villefranche, LOV, F-06230, Villefranche-sur-mer, France
[7]Aix Marseille Univ., CNRS, IRD, Université de Toulon, MIO UM 110, 13288, Marseille, France

Correspondence to: Antonio Tovar-Sánchez (a.tovar@csic.es)

Abstract

The Sea Surface Microlayer (SML) is known to be enriched in trace metals relative to the underlaying water and to harbor diverse microbial communities (i.e. neuston). However, the processes linking metals and biota in the SML are not yet fully understood. In this study, we analyzed the metal (Cd, Co, Cu, Fe, Ni, Mo, V, Zn and Pb) concentrations in aerosol samples, SML (dissolved and total fractions) and in subsurface waters (SSW; dissolved fraction at ~1 m depth) from the Western Mediterranean Sea during a cruise in May-June 2017. The bacterial community composition and abundance in the SML and SSW, and the primary production and Chl-a in the SSW were measured simultaneously at all stations during the cruise. Residence times of particulate metals derived from aerosols deposition ranged from a couple of minutes for Co (2.7 ± 0.9 min; more affected by wind conditions) to a few hours for Cu (3.0 ± 1.9 h). Concentration of most dissolved metals in both, the SML and SSW, were well correlated with the salinity gradient and showed the characteristic eastward increase in surface waters of the Mediterranean Sea (MS). Contrarily, the total fraction of some reactive metals in the SML (i.e. Cu, Fe, Pb and Zn) showed negative trends with salinity, these trends of concentrations seem to be associate to microbial uptake. Our results suggest a toxic effect of Ni on neuston and microbiology community's abundance of the top meter of the surface waters of the Western Mediterranean Sea.

Biogeosciences
Discussions

1. Introduction

The Mediterranean Sea (MS) is enriched in many trace metals relative to similar nutrient- depleted waters in the open ocean (e.g. Cd, Cr, Co, Cu, Ni, Fe, Zn) (Bonnet et al., 2013; Boyle et al., 1985; Sarthou and Jeandel, 2001; Sherrell and Boyle, 1988). The enrichment of metals in surface water has been associated to different sources including atmospheric deposition, river inflows, groundwaters, anthropogenic sources and the Atlantic Ocean inflow through the Gibraltar Strait (Boyle et al., 1985; Elbaz-Poulichet et al., 2001; Migon, 2005; Trezzi et al., 2016). The MS has one of the highest rates of aeolian deposition in the world with strong pulses of mineral dust from Africa, in addition to consistent anthropogenic aerosol inputs from Europe. Therefore, atmospheric deposition, dry and wet, is the dominant pathway for large scale transport of trace metals to the water column and sediments in MS (Guieu et al., 2002, 2010; Jordi et al., 2012; Ternon et al., 2010; Tovar-Sánchez et al., 2010, 2014). Many of these metals play an important role in biogeochemical processes of this sea. For example, it has been hypothesized that the high Co concentrations in the MS stimulate "de novo" synthesis of vitamin B_{12} as Co is the central metal ion in the B_{12} molecule (Bonnet et al., 2013). Although present in higher concentration than in other oceans, Fe has been considered as an important factor controlling phytoplankton growth (Sarthou and Jeandel, 2001). Copper from aerosol depositions has been demonstrated to have toxic effects on marine phytoplankton (Jordi et al., 2012; Paytan et al., 2009) while Ni and Zn have been considered as good geochemical tracers of aerosols impact in *Posidonia oceanica* (Tovar-Sánchez et al., 2010).

Studying the Sea-Surface Microlayer (SML), especially in a region dominated by aeolian deposition, is crucial for understanding trace metal dust solubility, ocean distribution, and the processes influencing the primary production and the vertical particle fluxes in the water column. The SML is considered the skin of the ocean as it serves as a boundary layer between the atmosphere and the ocean. With a thickness of 1−1000 μm, it is a prevalent feature of the surface ocean that shows distinct physical, chemical, and biological properties than the rest of the water column. This sea-air interface plays a key role in regulating the exchanges of gases, solutes and energy between water and atmosphere and is central to a wide range of global biogeochemical and climate regulation processes (Cunliffe et al., 2013).

Characterized by the dominated abundance of microorganisms (called neuston and ranging from bacteria to larger siphonophores (Wurl et al., 2017)), the SML is a particular marine ecosystem ecologically regulated. Although neuston in SML is formed by recruitment from the underlying plankton, its composition and activities are different and conditioned by meteorological conditions, intensity of UV radiation, organic matter content and/or aerosol impact among others (Cunliffe et al., 2013; Engel et al., 2017).

Impacted by different allochthonous sources (e.g. aerosols, ice, rivers) the SML is enriched in reactive trace metals (e.g. Cu, Fe, Pb) which metal stoichiometry signature is different from underlaying waters (Tovar-Sánchez et al., 2019). For example, in regions under the influences of dust events such as the North Atlantic Ocean or Mediterranean Sea, concentrations of Cu, Fe or Pb in the SML increase by a factor of up to 800, 200 and 150 times compared with the underlaying water (Tovar-Sánchez et al., 2019). It has been estimated that the SML in the MS contents around 2 tons of total Fe, and this amount could be much higher during episodes of dust event (Tovar-Sánchez et al., 2014). However, despite of such enrichment in trace metals concentrations, little is known about their residence times, their influence on the active microbial community within the SML, or their release rates towards the underlaying waters. Previous studies, from field sampling and laboratory microcosms, have estimated the residence times of dissolved and particulate trace metals (e.g. Al, Fe, Mn, Ni, Cu, Zn, and Pb) in the SML to range from a few minutes to a few hours. This is likely long enough to be chemically and biologically alter the SML and affect the composition and activity of the neuston community (Ebling and Landing, 2017; Hardy et al., 1985). However, estimates of residence times considering a variety of key field measurements that directly affect the physical, chemical and biological composition of the surface microlayer, such as dry and wet deposition fluxes, wind speeds, and neuston composition, have not been addressed yet.

Here, we studied the dissolved (<0.22 μm) and particulate trace metal composition (Cd, Co, Cu, Fe, Ni, Mo, V, Zn and Pb) of the SML in the central and Western MS. Aerosols were sampled and analyzed for trace metals at the same stations and residence time of particulate aerosol metals in the SML calculated. We analyzed the microbial composition and abundance in the SML and subsurface water (SSW), and the primary production and Chl-a concentration in the subsurface water (1-5m), and examined the relationships with trace metals concentration and distribution.

2. Material and Methods

Samples from SML, SSW and aerosols were collected during the cruise PEACETIME (ProcEss studies at the Air-sEa Interface after dust deposition in the MEditerranean sea) on board the French R/V 'Pourquoi Pas?' in the MS, from May 10th to June 11th, 2017. Twelve stations were sampled (Figure 1). Three of these stations were sampled twice (TYR 1-2, ION 1-2) or five times (FAST 1-5) at different days, counting for a total of 17 groups of samples (Table 1).

2.1. Aerosol sampling and analysis

The PEGASUS container was installed aboard the R/V Pourquoi Pas?, this container is a mobile platform equipped with a set of instruments optimized to collect and analyze in real time, gaseous compounds and particles in the atmospheric boundary layer (Formenti et al., 2019). Atmospheric sampling was performed using isokinetic and wind-oriented aerosol multi-samplers with a total sampled flow rate around 400 L min^{-1} per inlet. This inlet was developed for sampling both fine and coarse particles, with particles of aerodynamic diameter of about 40 µm (Rajot et al., 2008). This total flow was subdivided to various transmission lines which served the majority of the instrumentation. The aerosol size distribution from 10 nm to 30 µm was measured by a combination of standard optical and electrical mobility analyzers. The total mass concentration was obtained by an on-line Tapering Element Oscillating Microbalance (TEOM, model 1400a, Rupprecht and Patashnick).

One of the sampling lines was equipped with filtration unit to collect the aerosols on 47-mm polycarbonate membranes of 0.4 µm pore size (Whatman Nuclepore ™). The volume flow rate was set at 20 L.min^{-1}. All the filters were previously cleaned by immersion in ultrapure HCl (2%) during 2 hours and rinsing with ultrapure waters. A sampling strategy was made to avoid the contamination by the cruise smoking, firstly when the vessel was in station, the R/V was systematically positioned such as inlets were facing the wind (PEGASUS container and boat's chimney are on the opposite side of the deck). On the route, contamination-free sampling was operated when the relative wind direction was not in the direction of chimney exhaust. In total, 36 series of filters were collected which 17 filters during the stations and 5 blanks of filters were also prepared. The sampling locations for each filter is presented in Figure 1.

Aerosols filters were first analyzed by X-ray fluorescence spectrometry (SFX, spectrometer PW-2404, Panalytical™) for measuring chemical markers of particles origin sources (as Al and Ca). Filters were then leached by ultrapure water in order to determine the soluble fraction of metals. Finally, the filters were mineralized using an acid digestion protocol adapted from (Heimburger et al., 2013) in order to

5   quantify the insoluble (particulate) fraction of metals. The dissolved and digested samples were analyzed by HR-ICP-MS (Neptune Plus, Thermo Scientific ™) for trace metals: Cd, Co, Cr, Cu, Fe, Mn, Mo, Nd, Ni, Pb, V, Zn. The total concentration of metals corresponds to the sum of dissolved and particulate fraction of metals. Rain sampling was also operated during the cruise with on-line filtration collector (0.2µm, polycarbonate, Nuclepore Whatman™) (Heimburger et al., 2013) and the analysis of particulate

10 and dissolved metals were carried out by HR-ICP-MS.

2.2. Water sampling and analysis

2.2.1. Trace metals

Surface samples, i.e. SML and subsurface water (SSW: ~1 m depth), were collected from a

15 pneumatic boat deployed 0.5 – 1 mile away from the research vessel in order to avoid contamination of the samples from the vessel's influence. SML samples were collected using a glass plate sampler (Stortini et al., 2012; Tovar-Sánchez et al., 2019) which had been previously cleaned with acid overnight and rinsed thoroughly with ultrapure water (MQ-water). The 39 x 25 cm silicate glass plate had an effective sampling surface area of 1950 cm^2 considering both sides. In order to check for procedural contamination,

20 we collected SML blanks in some stations on board of the pneumatic boat by rinsing the glass plate with ultra-pure water and collecting 0.5 L using the glass plate system. The surface microlayer thickness was calculated following the formula of Wurl (2009) (Wurl, 2009). Total fraction of SML (i.e. T-SML) were directly collected from the glass plate system without filtration in a 0.5 L acid cleaned LDPE bottles, while that the dissolved fraction in the SML (i.e. D-SML) was rapidly filtered on board the pneumatic

25 boat through an acid-cleaned polypropylene cartridge filter (0.22µm; MSI, Calyx®). SSW were collected using an acid-washed Teflon tubing connected to a peristaltic pump and directly filtered on the same cartridge to collect the dissolved fraction (D-SSW). All samples were acidified on board to pH< 2 with Ultrapure-grade HCl in a class-100 HEPA laminar flow hood. Metals (i.e. Cd, Co, Cu, Fe, Ni, Mo, V, Zn

and Pb) were pre-concentrated using an organic extraction method (Bruland et al., 1979) and quantified by ICP-MS (Perkin Elmer ELAN DRC-e). Prior to the preconcentration and for the breakdown of metal-organic complexes and the removal of organic matter (Achterberg et al., 2001; Milne et al., 2010), total fraction samples (i.e. T-SML) were digested using an UV system consisting in one UV (80 W) mercury lamp that irradiated the samples (contained in quartz bottles) during 30 min. The accuracy of the pre-concentration method and analysis for trace metals was established using Seawater Reference Material for Trace Elements (CASS 6, NRC-CNRC) with recoveries ranging from 89% for Mo to 108% for Pb.

2.2.2. Ancillary parameters

Temperature and Salinity of surface seawater were measured with the underway thermosalinograph (TSG) system of the R/V Pourquoi Pas? which was composed of a *Seabird® SBE 21 seaCAT* associated to a *SBE 38* thermometer situated at the seawater inlet. The seawater inlet was situated 3 meters under the sea surface. The wind speed at 10 meters was measured with a *Gill Windsonic* ultrasonic anemometer from the on-board BATOS station deployed by the French meteorological agency *Météo France* on the vessel. Temperature, salinity and wind data were averaged on 30 seconds timelapses by the ship data management system TECHSAS (*TECHnical Sensor Acquisition System*). Average values of temperature, salinity and wind speed on a time period of 1 hour around the time of SML sampling are reported in table 1.

2.3. Biological sampling and analysis

2.3.1. Neuston

Microorganism inhabiting the SML are collectively referred to as the "neuston" (Engel et al., 2017). At the same time than trace metal samples collection, microorganism in the SML were sampled also using a glass plate system (50 x 26 cm silicate glass plate with an effective sampling surface area of 2600 cm^2 considering both sides). The water from the SSW was manually collected in acid clean borosilicate bottles at around 20 cm depth. Bacterial numbers were determined using flow cytometry from a 4 mL sample that was fixed with 200 mL glutaraldehyde (GDA, 1% final concentration). Samples were stored at -20 ºC for at most 2.5 months until analysis and were stained with SYBR Green I (Molecular

Probes) prior to quantification using a flow cytometer equipped with a 488 nm laser (Becton & Dickinson FACScalibur). A plot of side scatter (SSC) vs. green fluorescence (FL1) was used to detect the unique signature of the bacterial cells. The internal standard consisted of yellow-green latex beads (Polysciences, 0.5 mm). Abundance and area of Transparent Exopolymer Particles (TEP) were measured microscopically following a previously described method (Engel, A., 2009).

2.3.2. Phytoplankton and Primary Production

Chl-a concentration and primary production were measured in the SSW at 5 m depth. Primary production was measured with the ^{14}C-uptake technique. Seawater samples, collected from Niskin bottles at dawn, were dispensed into four (3 light and 1 dark) polystyrene bottles of 70 mL in volume, which were amended with 15 µCi of NaH^{14}CO$_3$ and incubated for 24 h inside a deck incubator refrigerated with surface seawater from the continuous water supply. The incubator was covered with a neutral density filter that provided an irradiance level of 70% of incident PAR. After incubation, samples were filtered, using low vacuum pressure, through 0.2-µm polycarbonate filters, which were exposed to HCl fumes overnight to remove non-fixed, inorganic ^{14}C. After adding 5 mL of liquid scintillation cocktail to the filters, the radioactivity on each sample was determined on-board with a liquid scintillation counter. To compute the rates of carbon fixation, the dark-bottle DPM value was subtracted from the light-bottle DPM value and a value of 26,000 µgC L^{-1} was used for the concentration of dissolved inorganic carbon. Chla concentratios were measured by HPLC (HPLC Agilent Technologies 1200) following the method described by Ras et al. (2008) (Ras et al., 2008).

2.4. Statistical analyses

Spearman rank correlation coefficient (r_s) was used to determine significant relationships ($p < 0.05$) between the parameters measured in the different compartments (air, SML and SSW) and parameters. Coefficient of determination (R^2) between the selected parameters were also calculated in order to determine how well correlations fit with a linear regression relationship. Statistical analysis was performed with the aid of the statistical software package SPSS 25.

3. Results and Discussion

3.1. Aerosols deposition

Metal aerosols composition is shown in Table 1. Average concentrations in our study were in the same order of magnitude, than previous measurements collected in the same region and season (Becagli et al., 2012; Calzolai et al., 2015; Tovar-Sánchez et al., 2014), and hence were consistent with Western Mediterranean background concentrations. No clear gradient (North-South or East-West) in atmospheric metals concentrations was observed during the cruise. Here, metal aerosols composition was mainly influenced by air masses from North of Europe and Atlantic Ocean (Figure S1), except between June 1st and June 4th, i.e for the stations St 9 and Fast 1-4 where African air masses loaded by dust were observed (Figure S1-2). During this period, the aerosol mass concentrations were the highest observed during the cruise with a maximum around 25 µg.m^{-3}, nevertheless these concentrations were typical of a moderate dust event (Pey et al., 2013). Aerosol Fe concentrations were the highest measured during the cruise, in average 245 ng.m^{-3} during this period. The same observation was done for Co. A good correlation between Ni and V in the collected aerosols all along the cruise, suggest a common source associated to heavy oil combustion; i.e. marine ship traffic (Becagli et al., 2012). Some rains occurred during the cruise, but only one was measured when the vessel was in station, June 5th from 2:36 am to 3:04 am between Fast 3 and Fast 4 samples. However, all the zone around the Fast station was rainy from the 3rd of June (Figure S3). As the collected rain composition was typical to dust wet deposition with high particulate concentrations of Al, Fe and Ca (Fu et al., in preparation), we suppose the rain-out of dust in the atmospheric column around this station occurred between the 3rd to the 5th of June.

3.2. Biochemical composition and distribution of the surface water

Trace metals concentrations in the surface waters of the MS varied depending on the compartmentation (i.e. SML or SSW) and along a longitudinal gradient (Table 1).

3.2.1. Trace metals in the SML

Trace metals concentrations of T-SML (Table 1) were lower, although, with the exception of Pb, of the same order of magnitude than those measured in the previous studies carried out in the MS (Tovar-

8

Sánchez et al., 2014). This lower content of metals in the SML is likely related with the lower dust aerosol's deposition during our sampling period and by the lack of influence of desert dust aerosols except for Fast station. T-SML concentration of Pb (average 663 ± 320 pM) was one order of magnitude lower than in previous studies impacted by pulses of both mineral African dust and anthropogenic aerosols coming from Europe (5596 ± 1589 pM) (Tovar-Sánchez et al., 2014). The highest concentrations of some metals were measured at the station FAST-3 (Co: 773,6 pM; Cu: 20.1 nM; Fe: 1433.3 nM and Pb: 1294.7 pM), likely impacted by the dusty rain events on this area.

Dissolved concentrations of Co, Zn, Pb, Cu and Ni showed a decreasing trend from the SML to the SSW, with concentrations 10.4 ± 0.7; 9.3 ± 5.5; 4.2 ± 1.8; 3.1 ± 1.5; and 1.2 ± 0.1 times higher in the SML than in the SSW, respectively. Vanadium (1.2 ± 0.42) and Fe (1.3 ± 1.5) varied lightly between SML and underlayer water, and Mo (1.0 ± 0.1) did not showed any differences (Table 1). Only Cd concentrations were consistently lower in the SML compared to the underlayer water (0.8 ± 0.2 times lower). Such depletion of dissolved metals in the SML compared to the underlayer water has been previously observed in areas with no significant aerosols inputs (Ebling and Landing, 2015, 2017). Although not fully understood, some mechanisms such as dominance of removal mechanisms versus diffusion, or higher influence of underlaying metal sources have been previously suggested to explain this metal depletion (Ebling and Landing, 2017; Hunter, 1980).

Spatial distribution of Co and Ni concentrations in the D-SML were well correlated with those measured in the D-SSW (Spearman's correlation coefficient (r_s): 0.87 for Co and 0.91 for Ni; p<0.01, Table 2), indicating for these elements an efficient diffusive mixing between these two compartments. These elements were also well correlated with the surface salinity distribution (r_s: 0.62 for Co and 0.93 for Ni; p<0.01, Table 2), and presented an eastward trend of increasing concentration, which is consistent with the characteristic distribution of metals on the surface of the MS (see section 3.2.4. below). Variations in concentrations for the rest of the elements (i.e. Cd, Cu, Fe, Pb, V and Zn) in the D-SML were not correlated either with the underlayer water or salinity gradient. Multiple physical, chemical and biological processes taking place in the SML could be affecting and controlling the mobility and diffusion of these elements between compartments. However, the concentrations of Cu, Fe and Zn in the T-SML showed an opposite trend with a longitudinal gradient inversely correlated with the salinity (r_s: -0.59 for

Cu; -0.69 for Fe, and -0.61 for Zn; p<0.01, Table 2). Since aerosols metal concentrations did not show any longitudinal trend and no other natural or anthropogenic sources were identified in the region, gradient concentration of these reactive trace elements in the T-SML must be influenced by other factors different than sources inputs, water exchange or dilution with Atlantic waters.

5

3.2.2. Residence time of trace metals in the SML

Estimates of the residence times of metals from aerosols inputs in the SML are critical to better understand the biogeochemical processes that affect the fate and distribution of trace metals in the surface ocean. To estimate the residence time (t) of particulate metals in the SML, we used the equation proposed
10 by Ebling and Landing (2017) (Ebling and Landing, 2017):

$t= [TE]_{SML} \times d/J_{aerosol}$

where $[TE]_{SML}$ is the concentration of trace element (TE) in the T-SML, d is the thickness of the SML and, and $J_{aerosol}$ is the measured aerosol trace metal flux. $J_{aerosol}$ was estimated by multiplying the metals aerosol concentrations with the sedimentation velocity, which is dependent on aerosols size. Thus, we
15 used a velocity of mineral dust deposition for Fe (1 cm.s^{-1}) and an average velocity of fine anthropogenic particles for the other metals, i.e. 0.1 cm.s^{-1} (Baker et al., 2010; Duce et al., 1991). For the calculations of the residence times along our different stations we used simultaneous empirical measurements of metals concentrations in the SML and metals aerosol fluxes (Table 3). Residence time of particulate metals (T-SML) ranged from 12 min for Co and Fe to 7.6 h for Cu. Since Mo and Cd are not enriched in the SML
20 they were not considered in this calculation. Although variable among stations, residence time of Cu (3.0 ± 1.9 h), Zn (2.1 ± 0.8 h), V (1.7 ± 0.4 h), Pb (1.4 ± 0.7 h), Ni (55 ± 14 min), Fe (5.0 ± 3.1 min, excluding the station Fast 3) and Co (2.7 ± 0.9 min, excluding the station Fast 3) were relatively consistent with previous estimates in regions under low aerosols inputs (Ebling and Landing, 2017). Our results indicate that Fast 3 station was affected by the dusty rain events, which increased the concentration of some metals
25 in the T-SML. Iron and Co were the elements that increased the most with major impact on their residence time for that station, i.e. multiplied by a factor 10 (Table 3). On average, while the highest residence times obtained for Cu, Pb and Zn are in agreement with their strong affinity to particles and therefore with a high probability of retention in the SML, other reactive elements such as Co and Fe presented, the shortest

residence time. Since, such fast transfer of these particle metals to the underlayer water (in the order of 1-3 min) is unlikely (mainly due their affinities to organic ligands), and dissolution is not immediately reflected in an increase of concentration in the dissolved fraction (i.e. D-SML), other parameters (linked to dynamic or biological activity) would be affecting the residence time of these elements in the SML. In

5   the case of Co, wind seems to partly explain this short residence time. Wind speed showed high and significant negative correlation with the residence time of Co (r_s: -0.67, $p<0.01$), Ni (r_s: -0.76 $p< p<0.01$) and V (r_s: -0.80 $p< p<0.01$) in the SML, suggesting an influence of wind on the diffusion of these elements to the underlayer water (Table 2).

10   *3.2.3. Neuston composition*

       The microbial composition (Bacteria; High nucleid acid-content bacteria: HNA; Low nucleid acid-content bacteria: LNA; phytoplankton; phytoplankton small; phytoplankton middle; phytoplankton large; Small cyanobacteria like cells: CBL-small; middle-large cyanobacteria like cells: CBL-middle-large) and abundance in the SML are shown in Table 1. Bacterial abundance in the SML ranged from

15   $2x10^5$ to $1x10^6$ cell mL^{-1} (average: $5.1x10^5 \pm 2.2x10^5$ cell mL^{-1}) that is of the same order of magnitude than abundance measured in the SML of other regions (e.g. in the Peruvian Coast with average of $8.9x10^5 \pm 4.3x10^5$ cell mL^{-1}) (Zäncker et al., 2018). Bacterial community was dominated by low nucleid acid-content bacteria (LNA) with an average concentration of $2.8 \ x10^5 \pm 1.0x10^5$ cell mL^{-1}. In general, and with the exception of phytoplankton middle and CBL-small, microbial abundance was higher in the SML

20   than in the SSW with abundances ranging from 1 to 6 times higher for bacteria and CBL-middle-large, respectively (Table 1).

       A microbial abundance decreases from west to east related to the increasing oligotrophy (explained though an increased P limitation) of the surface Mediterranean waters has been described (Pulido-Villena E. et al., 2012). In this study, microbial abundance in the SML and T-SML reactive

25   elements (i.e. Cu, Fe, and Zn) showed the same longitudinal gradients with decreasing eastward concentration along the southern coast of the MS. In fact, bacterial abundances were significantly and positively correlated with these bioactive T-SML metals (i.e. r_s: Cu: 0.65 $p<0.01$; Fe: 0.53 $p<0.05$; and Zn: 0.49 $p<0.05$), suggesting that bacterioneuston could be affecting the concentration and fate of Cu, Fe

and Zn in the SML. Bacteria would efficiently assimilate the available fraction of Cu, Fe and Zn, resulting in a decrease and increase of the D-SML and T-SML fractions, respectively (Table 1). No general relationship between concentrations of metals and TEPs (high molecular weight polymers released by phytoplankton and bacteria and with high metal binding capacity (Passow, 2002)) were found in the SML,

5   although both showed strongly increased values after a dust deposition event at FAST 3 (Table 4). We therefore assume that metal assimilation by microbial communities would also explain the higher residence time of Cu and Zn (in the order of hours) in the SML. However, in the case of Fe with an estimated residence time of a few minutes, other processes different than wind speed and neuston uptake, should be contributing to facilitate the transfer from the SML to the underlayer water. For example,

10 photochemical reactions drive by intense solar radiation exposure in the SML could play an important role in the dissolution processes of this metal (Boyd et al., 2010). On the other hand, Ni was strongly and negatively correlated with bacteria abundance in the D-SML (r_s = -0.93, $p<0.01$; R^2 = 0.74, $p<0.01$) suggesting, contrarily to Cu, Fe and Zn, a possible inhibiting role on the microbiology growth (Table 4 and Figure 2) (see next section for more discussion).

15

3.2.4. Subsurface water

The D-SSW concentrations of Cd, Co, Cu, Ni, Mo and Zn showed a longitudinal gradient of concentrations increasing from west to east, with strong significant positive correlations with longitude for Cd, Co and Ni (Figure 3). This trend is consistent with previous studies where the increased eastward

20 concentration along the southern coast of the MS is indicated to be due to factors such as: more intense Saharan deposition on the eastern MS (Guieu et al., 2002); more rapid exchange of water masses and margin inputs in the Western part (Yoon et al., 1999) or, as suggested for Co, the regeneration of biogenic particulate eastward that yields a westward decreased of the dissolved Co in surface (Dulaquais et al., 2017). Since surface salinity showed the same eastward increase and was close correlated with those

25 metals (r_s ranged from 0.51 $p<0.05$ for Mo to 0.97 $p<0.01$ for Ni; Table 2), the exchange with the surface Atlantic Ocean waters seems to be the main cause of this gradient of concentrations in our study, although higher aerosol inputs in the western MS could also contribute to this gradient. Other metals (i.e. Fe, Pb and V) did not show any clear geographical trend and variations in surface concentrations could be

influenced by several factors other than dilution or exchange, such as vertical diffusive fluxes or, specific metal sources, as it is in the case of Fe and Pb that has been suggested to be more affected by atmospheric inputs (Nicolas et al., 1994; Yoon et al., 1999). In fact, Pb was the only element that showed significant positive correlation with latitude (r_s: 0.88 p<0.01, Table 2) suggesting an influence of the northern region

5   of the MS.

    D-SSW concentrations of Ni were strongly and negatively correlated with microbial abundance (mainly with heterotrophic bacterial) in the underlaying water (r_s : -0.91, p<0.01; $R^2 = 0.87$, p<0.01) (Figure 2 and Table 4) suggesting a potential negative role of this metal on bacteria and small phytoplankton on the top meter of the surface western MS, including the SML. Toxicity by Ni at

10   concentrations of ~50 nM has been previously demonstrated in the western MS, with inhibitions of 10% (EC_{10}) in phycoerythrin and Chl-a signals of natural population of the picoplankter *Synechococcus* sp. (Debelius et al., 2011). Although that toxicity concentration (tested in picoplankton), is around 13 time higher than average values measured in our samples (T-SML: 4.1 ± 0.5 nM, D-SML: 3.9 ± 0.6 nM and D-SSW: 3.2 ± 0.6 nM; Table 1), deleterious effects on the neuston and microbial communities to lower

15   concentrations could be feasible in the top meter of the surface sea. Indeed, UV radiations in this surface layer are highly intense and can acts as a biochemical microreactor where many transformations and photochemical reaction occurs (Wurl et al., 2017) affecting complexation, solubilization, bioaccumulation and/or toxicity of many trace elements. Even if a general decreasing trend from west to east of microbial abundance due to the increasing oligotrophy has been described, it is interesting to

20   mention that primary production and Chl-a concentration (measured a 5 m depth), did not show significant correlations with Ni (Table 4). We therefore assume that toxicity of Ni is mainly affecting the bacterial community and/or on the top meter of the surface ocean. Nickel, as other transition metals, is an essential cofactor of several enzymes, however, it becomes toxic when homeostasis fails. Multiple potential mechanisms of Ni toxicity to aquatic organisms, and in particular to bacteria, have been identified

25   (Macomber and Hausinger, 2016). Among the different possible toxicity mechanisms (including inhibition of Zn and Fe metalloenzymes and non-metalloenzymes) the toxicity involving reactive oxygen species (ROS) is likely the most feasible in surface seawater. While Ni itself is a poor generator of reactive oxygen species (ROS) when compared to other metals like Fe or Cu, its reactivity and ROS productions

can be enhanced by the displacement of redox-active iron from iron metallocenters (Macomber and Hausinger, 2016) or when chelated by oligopeptides and histidine (Brix et al., 2017), which are abundant in the SML. It appears that Nickel-dependent toxicity involving ROS may be likely mechanism of oxidative stress in marine microbial organism of the surface ocean. There is many information on the

5 effect of Ni on insolate laboratory microalgae experiments, however its toxicity role in oceans have been poorly explored. Therefore, additional studies on Ni diffusión from SML, solubility, speciation, and the effects on phytoplankton at the species level are required to fully understand the magnitude of this finding.

4. Conclusions

10 Our results show that the SML in the MS is enriched in trace metals relative to the SSW even under low aerosols deposition rates. While some metals entering in the SML (e.g. Cd, Co, Ni and V) show efficient diffusive mixing from SML to SSW, other more reactive metals such as Cu, Fe, Pb and Zn affected by chemical and biological processes show a major difficulty of mobility. A strong negative correlation between Ni concentration and heterotrophic bacterial abundance in the SML and SSW suggest an

15 inhibiting role of this element on the microbial growth in the top meter of the surface.

Biogeosciences
Discussions

Open Access

EGU

References

5 Achterberg, E. P., Braungardt, C. B., Sandford, R. C. and Worsfold, P. J.: UV digestion of seawater samples prior to the determination of copper using flow injection with chemiluminescence detection, Analytica Chimica Acta, 440(1), 27–36, doi:10.1016/S0003-2670(01)00824-8, 2001.

Baker, A. R., Lesworth, T., Adams, C., Jickells, T. D. and Ganzeveld, L.: Estimation of atmospheric
10 nutrient inputs to the Atlantic Ocean from 50°N to 50°S based on large-scale field sampling: Fixed nitrogen and dry deposition of phosphorus: ATLANTIC ATMOSPHERIC NUTRIENT INPUTS, Global Biogeochem. Cycles, 24(3), n/a-n/a, doi:10.1029/2009GB003634, 2010.

Becagli, S., Sferlazzo, D. M., Pace, G., di Sarra, A., Bommarito, C., Calzolai, G., Ghedini, C., Lucarelli,
15 F., Meloni, D., Monteleone, F., Severi, M., Traversi, R. and Udisti, R.: Evidence for heavy fuel oil combustion aerosols from chemical analyses at the island of Lampedusa: a possible large role of ships emissions in the Mediterranean, Atmos. Chem. Phys., 12(7), 3479–3492, doi:10.5194/acp-12-3479-2012, 2012.

Bonnet, S., Tovar-Sánchez, A., Panzeca, C., Duarte, C. M., Ortega-Retuerta, E. and Sañudo-Wilhelmy,
20 S. A.: Geographical gradients of dissolved Vitamin B12 in the Mediterranean Sea, Front Microbiol, 4, doi:10.3389/fmicb.2013.00126, 2013.

Boyd, P. W., Mackie, D. S. and Hunter, K. A.: Aerosol iron deposition to the surface ocean — Modes of
25 iron supply and biological responses, Marine Chemistry, 120(1–4), 128–143, doi:10.1016/j.marchem.2009.01.008, 2010.

Boyle, E. A., Chapnick, S. D., Bai, X. X. and Spivack, A.: Trace metal enrichments in the Mediterranean

Sea, Earth and Planetary Science Letters, 74(4), 405–419, doi:10.1016/S0012-821X(85)80011-X, 1985.

Brix, K. V., Schlekat, C. E. and Garman, E. R.: The mechanisms of nickel toxicity in aquatic environments: An adverse outcome pathway analysis: Adverse outcome pathway for Ni, Environ Toxicol Chem, 36(5), 1128–1137, doi:10.1002/etc.3706, 2017.

5

Bruland, K. W., Franks, R. P., Knauer, G. A. and Martin, J. H.: Sampling and analytical methods for the determination of copper, cadmium, zinc, and nickel at the nanogram per liter level in sea water, Analytica Chimica Acta, 105, 233–245, doi:10.1016/S0003-2670(01)83754-5, 1979.

10 Calzolai, G., Nava, S., Lucarelli, F., Chiari, M., Giannoni, M., Becagli, S., Traversi, R., Marconi, M., Frosini, D., Severi, M., Udisti, R., di Sarra, A., Pace, G., Meloni, D., Bommarito, C., Monteleone, F., Anello, F. and Sferlazzo, D. M.: Characterization of PM10 sources in the central Mediterranean, Atmos. Chem. Phys., 15(24), 13939–13955, doi:10.5194/acp-15-13939-2015, 2015.

15 Cunliffe, M., Engel, A., Frka, S., Gašparović, B., Guitart, C., Murrell, J. C., Salter, M., Stolle, C., Upstill-Goddard, R. and Wurl, O.: Sea surface microlayers: A unified physicochemical and biological perspective of the air–ocean interface, Progress in Oceanography, 109, 104–116, doi:10.1016/j.pocean.2012.08.004, 2013.

20 Debelius, B., Forja, J. M. and Lubián, L. M.: Toxicity of copper, nickel and zinc to Synechococcus populations from the Strait of Gibraltar, Journal of Marine Systems, 88(1), 113–119, doi:10.1016/j.jmarsys.2011.02.009, 2011.

Duce, R. A., Liss, P. S., Merrill, J. T., Atlas, E. L., Buat-Menard, P., Hicks, B. B., Miller, J. M., Prospero, 25 J. M., Arimoto, R., Church, T. M., Ellis, W., Galloway, J. N., Hansen, L., Jickells, T. D., Knap, A. H., Reinhardt, K. H., Schneider, B., Soudine, A., Tokos, J. J., Tsunogai, S., Wollast, R. and Zhou15, M.: The Atmospheric Input of Trace Species to the World Ocean, Global Biogeochem. Cycles, 5(3), PAGES 193–259, 1991.

Dulaquais, G., Planquette, H., L'Helguen, S., Rijkenberg, M. J. A. and Boye, M.: The biogeochemistry of cobalt in the Mediterranean Sea: Cobalt in the Mediterranean Sea, Global Biogeochemical Cycles, doi:10.1002/2016GB005478, 2017.

5

Ebling, A. M. and Landing, W. M.: Sampling and analysis of the sea surface microlayer for dissolved and particulate trace elements, Marine Chemistry, 177, 134–142, doi:10.1016/j.marchem.2015.03.012, 2015.
Ebling, A. M. and Landing, W. M.: Trace elements in the sea surface microlayer: rapid responses to changes in aerosol deposition, Elem Sci Anth, 5(0), doi:10.1525/elementa.237, 2017.

10

Elbaz-Poulichet, F., Guieu, C. and Morley, N. H.: A Reassessment of Trace Metal Budgets in the Western Mediterranean Sea, Marine Pollution Bulletin, 42(8), 623–627, doi:10.1016/S0025-326X(01)00065-0, 2001.

15 Engel, A.: Determination of marine gel particles, in Practical Guidelines for the Analysis of Seawater, vol. ed. O. Wurl (, pp. 125–142, Boca Raton FL: CRC Press Taylor & Francis Group)., 2009.

Engel, A., Bange, H. W., Cunliffe, M., Burrows, S. M., Friedrichs, G., Galgani, L., Herrmann, H., Hertkorn, N., Johnson, M., Liss, P. S., Quinn, P. K., Schartau, M., Soloviev, A., Stolle, C., Upstill-
20 Goddard, R. C., van Pinxteren, M. and Zäncker, B.: The Ocean's Vital Skin: Toward an Integrated Understanding of the Sea Surface Microlayer, Front. Mar. Sci., 4, 165, doi:10.3389/fmars.2017.00165, 2017.

Formenti, P., D'Anna, B., Flamant, C., Mallet, M., Piketh, S. J., Schepanski, K., Waquet, F., Auriol, F.,
25 Brogniez, G., Burnet, F., Chaboureau, J.-P., Chauvigné, A., Chazette, P., Denjean, C., Desboeufs, K., Doussin, J.-F., Elguindi, N., Feuerstein, S., Gaetani, M., Giorio, C., Klopper, D., Mallet, M. D., Nabat, P., Monod, A., Solmon, F., Namwoonde, A., Chikwililwa, C., Mushi, R., Welton, E. J. and Holben, B.: The Aerosols, Radiation and Clouds in southern Africa (AEROCLO-sA) field campaign in Namibia:

overview, illustrative observations and way forward, Bull. Amer. Meteor. Soc., BAMS-D-17-0278.1, doi:10.1175/BAMS-D-17-0278.1, 2019.

Guieu, C., Bozec, Y., Blain, S., Ridame, C., Sarthou, G. and Leblond, N.: Impact of high Saharan dust inputs on dissolved iron concentrations in the Mediterranean Sea: IMPACT OF HIGH SAHARAN DUST INPUTS, Geophysical Research Letters, 29(19), 17-1-17–4, doi:10.1029/2001GL014454, 2002.

Guieu, C., Loÿe-Pilot, M.-D., Benyahya, L. and Dufour, A.: Spatial variability of atmospheric fluxes of metals (Al, Fe, Cd, Zn and Pb) and phosphorus over the whole Mediterranean from a one-year monitoring experiment: Biogeochemical implications, Marine Chemistry, 120(1–4), 164–178, doi:10.1016/j.marchem.2009.02.004, 2010.

Hardy, J. T., Apts, C. W., Crecelius, E. A. and Fellingham, G. W.: The sea-surface microlayer: Fate and residence times of atmospheric metals1: Surface microlayer metals, Limnol. Oceanogr., 30(1), 93–101, doi:10.4319/lo.1985.30.1.0093, 1985.

Heimburger, A., Losno, R. and Triquet, S.: Solubility of iron and other trace elements in rainwater collected on the Kerguelen Islands (South Indian Ocean), Biogeosciences, 10(10), 6617–6628, doi:10.5194/bg-10-6617-2013, 2013.

Hunter, K. A.: Processes affecting particulate trace metals in the sea surface microlayer, Marine Chemistry, 9(1), 49–70, doi:10.1016/0304-4203(80)90006-7, 1980.

Jordi, A., Basterretxea, G., Tovar-Sánchez, A., Alastuey, A. and Querol, X.: Copper aerosols inhibit phytoplankton growth in the Mediterranean Sea, PNAS, 201207567, doi:10.1073/pnas.1207567110, 2012.

Macomber, L. and Hausinger, R. P.: Nickel Toxicity, Regulation, and Resistance in Bacteria, in Stress

Biogeosciences Open Access

Discussions

EGU

and Environmental Regulation of Gene Expression and Adaptation in Bacteria, edited by F. J. de Bruijn, pp. 1131–1144, John Wiley & Sons, Inc., Hoboken, NJ, USA., 2016.

Migon, C.: Trace Metals in the Mediterranean Sea, in The Mediterranean Sea, edited by A. Saliot, pp.
5   151–176,   Springer   Berlin   Heidelberg.   [online]   Available   from: http://link.springer.com/chapter/10.1007/b107146 (Accessed 26 November 2013), 2005.

Milne, A., Landing, W., Bizimis, M. and Morton, P.: Determination of Mn, Fe, Co, Ni, Cu, Zn, Cd and Pb in seawater using high resolution magnetic sector inductively coupled mass spectrometry (HR-ICP-
10   MS), Analytica Chimica Acta, 665(2), 200–207, doi:10.1016/j.aca.2010.03.027, 2010.

Nicolas, E., Ruiz-Pino, D., Buat-Ménard, P. and Bethoux, J. P.: Abrupt decrease of lead concentration in the Mediterranean sea: A response to antipollution policy, Geophys. Res. Lett., 21(19), 2119–2122, doi:10.1029/94GL01277, 1994.
15

Passow, U.: Transparent exopolymer particles (TEP) in aquatic environments, Progress in Oceanography, 55(3–4), 287–333, doi:10.1016/S0079-6611(02)00138-6, 2002.

Paytan, A., Mackey, K. R. M., Chen, Y., Lima, I. D., Doney, S. C., Mahowald, N., Labiosa, R. and Post,
20   A. F.: Toxicity of atmospheric aerosols on marine phytoplankton, PNAS, 106(12), 4601–4605, doi:10.1073/pnas.0811486106, 2009.

Pey, J., Querol, X., Alastuey, A., Forastiere, F. and Stafoggia, M.: African dust outbreaks over the Mediterranean Basin during 2001-2011: PM10; concentrations, phenomenology and trends, and its
25   relation with synoptic and mesoscale meteorology, Atmos. Chem. Phys., 13(3), 1395–1410, doi:10.5194/acp-13-1395-2013, 2013.

Pulido-Villena E., Ghiglione J.F, Ortega-Retuerta E, Van-Wambeke F and Zohary T: Heterotrophic

bacteria in the pelagic realm of the Mediterranean Sea, in Life in the Mediterranean Sea: a look at habitat changes, pp. 227–266, Nova Publishers., 2012.

Rajot, J. L., Formenti, P., Alfaro, S., Desboeufs, K., Chevaillier, S., Chatenet, B., Gaudichet, A., Journet, E., Marticorena, B., Triquet, S., Maman, A., Mouget, N. and Zakou, A.: AMMA dust experiment: An overview of measurements performed during the dry season special observation period (SOP0) at the Banizoumbou (Niger) supersite, J. Geophys. Res., 113, D00C14, doi:10.1029/2008JD009906, 2008.

Ras, J., Claustre, H. and Uitz, J.: Spatial variability of phytoplankton pigment distributions in the Subtropical South Pacific Ocean: comparison between in situ and predicted data, 17, 2008.

Sarthou, G. and Jeandel, C.: Seasonal variations of iron concentrations in the Ligurian Sea and iron budget in the Western Mediterranean Sea, Marine Chemistry, 74(2–3), 115–129, doi:10.1016/S0304-4203(00)00119-5, 2001.

Sherrell, R. M. and Boyle, E. A.: Zinc, chromium, vanadium and iron in the Mediterranean Sea, Deep Sea Research Part A. Oceanographic Research Papers, 35(8), 1319–1334, doi:10.1016/0198-0149(88)90085-4, 1988.

Stortini, A. M., Cincinelli, A., Degli Innocenti, N., Tovar-Sánchez, A. and Knulst, J.: 1.12 - Surface Microlayer, in Comprehensive Sampling and Sample Preparation, edited by Editor-in-Chief: Janusz Pawliszyn, pp. 223–246, Academic Press, Oxford. [online] Available from: http://www.sciencedirect.com/science/article/pii/B9780123813732000181 (Accessed 1 October 2012), 2012.

Ternon, E., Guieu, C., Loÿe-Pilot, M.-D., Leblond, N., Bosc, E., Gasser, B. and Miquel, J.-C.: The impact of Saharan dust on the particulate export in the water column of the North Western Mediterranean Sea, Biogeosciences Discuss., 6(6), 10737–10773, 2010.

Tovar-Sánchez, A., Serón, J., Marbà, N., Arrieta, J. M. and Duarte, C. M.: Long-term records of trace metal content of western Mediterranean seagrass (Posidonia oceanica) meadows: Natural and anthropogenic contributions, J. Geophys. Res., 115, 10 PP., doi:201010.1029/2009JG001076, 2010.

5

Tovar-Sánchez, A., Arrieta, J. M., Duarte, C. M. and Sañudo-Wilhelmy, S. A.: Spatial gradients in trace metal concentrations in the surface microlayer of the Mediterranean Sea, Front. Mar. Sci., 1, doi:10.3389/fmars.2014.00079, 2014.

10 Tovar-Sánchez, A., González-Ortegón, E. and Duarte, C. M.: Trace metal partitioning in the top meter of the ocean, Science of The Total Environment, 652, 907–914, doi:10.1016/j.scitotenv.2018.10.315, 2019.
Trezzi, G., Garcia-Orellana, J., Rodellas, V., Santos-Echeandia, J., Tovar-Sánchez, A., Garcia-Solsona, E. and Masqué, P.: Submarine groundwater discharge: A significant source of dissolved trace metals to the North Western Mediterranean Sea, Marine Chemistry, 186, 90–100,
15 doi:10.1016/j.marchem.2016.08.004, 2016.

Wurl, O.: Practical Guidelines for the Analysis of Seawater, 1st ed., CRC Press., 2009.

Wurl, O., Ekau, W., Landing, W. M. and Zappa, C. J.: Sea surface microlayer in a changing ocean – A
20 perspective, Elem Sci Anth, 5(0), 31, doi:10.1525/elementa.228, 2017.

Yoon, Y.-Y., Martin, J.-M. and Cotté, M. H.: Dissolved trace metals in the Western Mediterranean Sea: total concentration and fraction isolated by C18 Sep-Pak technique, Marine Chemistry, 66(3–4), 129–148, doi:10.1016/S0304-4203(99)00033-X, 1999.

25

Zäncker, B., Cunliffe, M. and Engel, A.: Bacterial Community Composition in the Sea Surface Microlayer Off the Peruvian Coast, Front. Microbiol., 9, 2699, doi:10.3389/fmicb.2018.02699, 2018.

Figure 1. Location of the sampling stations in the studied region.
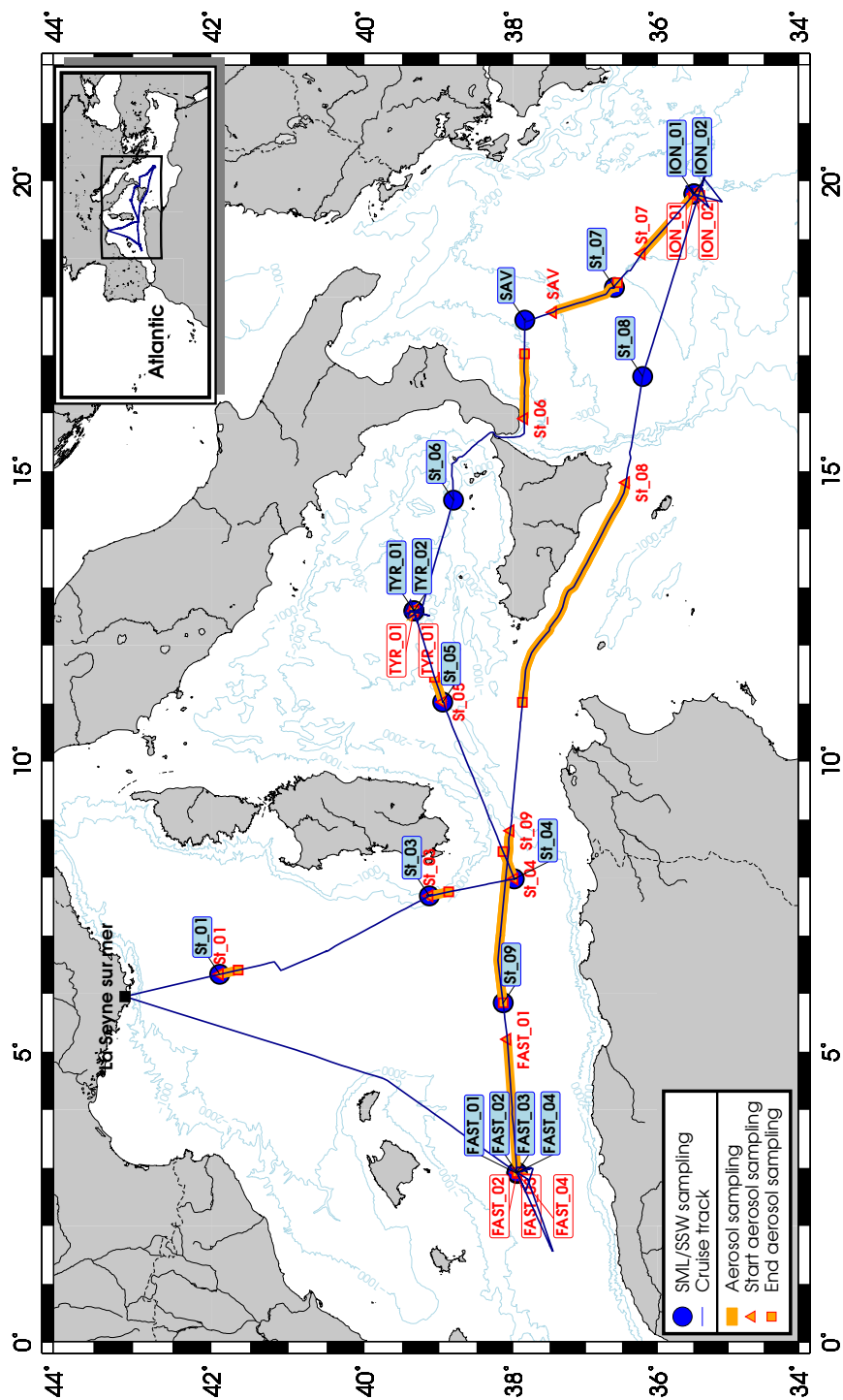
Figure 2. Concentration of Dissolved Ni plotted against bacterial abundance in the SML (black dots) and in the Subsurface water (red open dots). The lines represent linear regression equations.

5
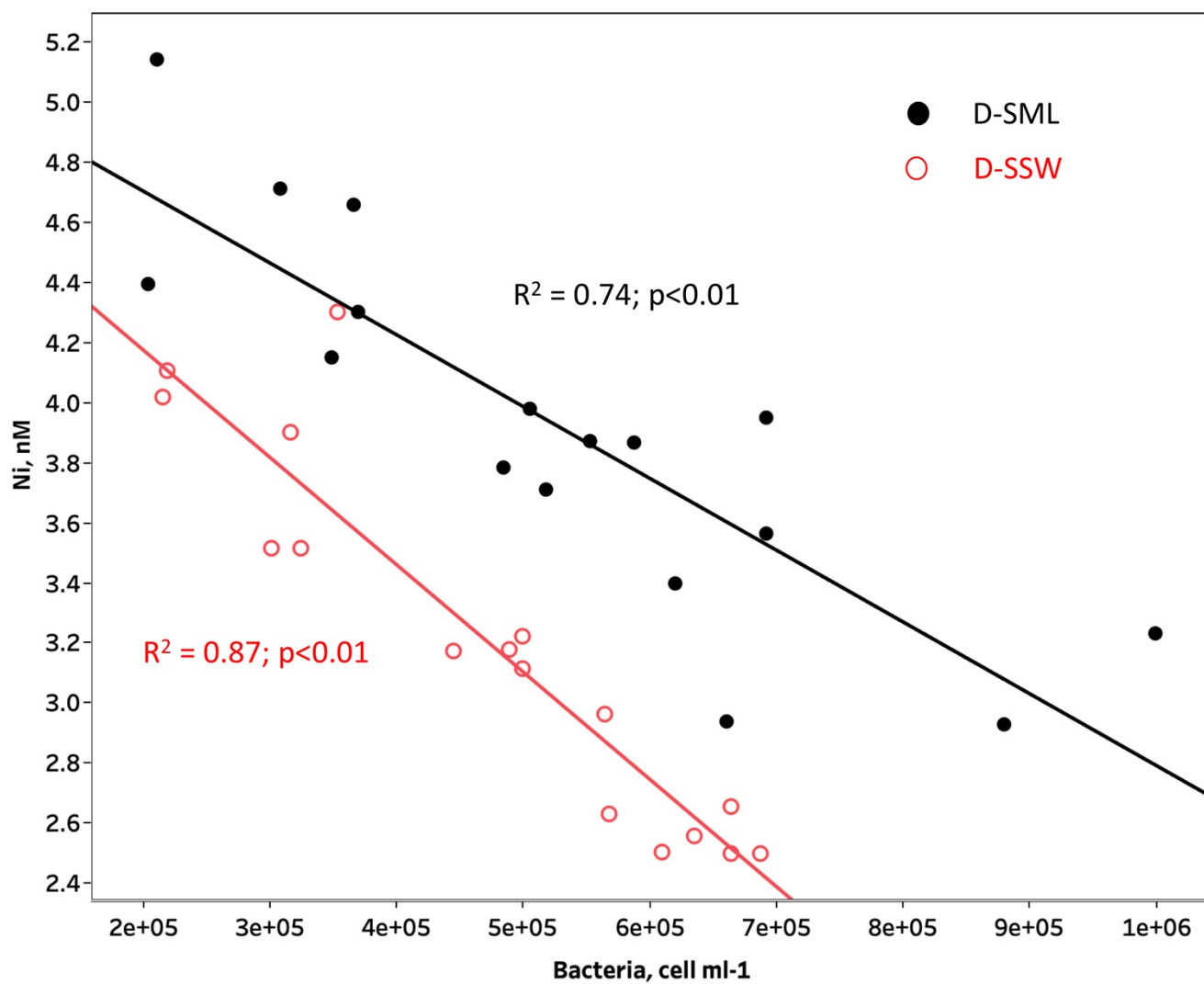
Figure 3. Salinity and dissolved trace metals concentration in the subsurface waters plotted against longitude. The dashed lines represent linear regression equations.

5

Table 1. Parameters measured in all stations. Metals in pmol.m⁻³ or nmol.m⁻³ for aerosols and nM or pM in water compartments.

Station	Date	Time UTC	Lat	Long	Wind Speed knots	Salinity 5m PSU	Temp 5m °C	Sample	Cd nM·ng·m⁻³	Co pM·ng·m⁻³	Cu pM·ng·m⁻³	Fe nM·ng·m⁻³	Mo nM·ng·m⁻³	Ni nM·ng·m⁻³	Pb pM·ng·m⁻³	V nM·ng·m⁻³	Zn nM·ng·m⁻³	Bacteria cell·ml⁻¹ x10⁵	Bacteria HNA x10⁵	Bacteria LNA x10⁵	Phyto cell·ml⁻¹ x10²	Phyto small x10²	Phyto middle x10²	Phyto large cell·ml⁻¹	CbL small cell·ml⁻¹	CbL middle-large cell·ml⁻¹	TEP particles·l⁻¹ x10⁶	PP mgC·m⁻³·d⁻¹	Chl-a µg·l⁻¹
St. 1	12/5/17	13:15	41.8918	6.3333	18.8	38.2	16.4	Aerosol	0.1	0.1	2.0	37.9	0.4	2.7	1.1	8.0	3.6												
								D-SML	74.0	109.8	8.0	6.8	125.9	4.1	323.0	14.9	8.0	3.49	1.62	1.88	84.71	7.51	29.85	3.43	3685.32	1080.89	7.67	5.555	0.187
								T-SML	76.3	112.6	3.6	81.8	121.0	4.5	1217.5	21.7	11.1	3.02	1.26	1.78	70.74	8.34	33.70	6.86	2707.37	192.16	4.79		
								SSW	78.5	11.3	1.6	14.3	130.1	3.5	111.0	23.0	1.9												
St. 3	14/5/17	5:30	39.1333	7.6835	5.6	37.2	18.7	Aerosol	0.0	0.1	0.4	22.9	0.0	2.4	0.3	6.5	3.3												
								D-SML	62.7	159.6	5.8	3.7	132.5	4.0	766.0	10.6	8.5	5.06	1.80	3.30	30.76	16.88	5.78	3.44	10.32	832.13	8.24		
								T-SML	72.5	163.1	7.5	72.2	124.9	4.0	858.2	25.4	12.4	5.68	2.10	3.62	21.72	14.89	5.88	0.00	17.19	113.47	1.50	1.613	0.095
								SSW	69.3	13.6	1.2	2.3	124.3	2.6	83.6	23.8	0.6												
St. 4	15/5/17	7:30	37.9832	7.9768	6.8	37.1	19.8	Aerosol	0.0	0.1	0.5	27.3	0.1	2.9	0.2	6.8	2.6												
								D-SML	57.0	143.3	5.5	1.5	121.7	3.6	601.5	15.2	14.7	6.92	3.58	3.37	31.11	17.71	5.28	0.00	10.29	837.26	5.97		
								T-SML	59.7	172.0	12.5	32.6	122.4	4.0	881.3	27.1	12.6	6.65	3.59	3.10	24.35	16.02	7.14	0.00	17.16	137.26	2.66	1.709	0.090
								SSW	65.0	15.1	7.2	5.4	125.0	2.7	87.4	18.4	0.7												
St. 5	16/5/01	6:00	38.9532	11.023	15.5	37.8	19.9	Aerosol	0.0	0.1	0.6	57.3	0.4	1.9	0.7	3.9	2.6												
								D-SML	66.0	143.0	2.6	0.6	122.6	4.0	212.7	35.0	4.7	4.27	2.05	2.25	16.76	8.77	3.37	0.00	3.44	495.15	4.55		
								T-SML	64.4	152.9	4.8	37.4	128.6	3.9	559.3	31.1	11.1	4.45	2.12	2.36	13.74	7.98	5.02	0.00	17.19	92.84	2.28	1.642	0.060
								SSW	n.m	13.8	1.8	2.0	130.7	3.2	101.2	18.7	1.2												
TYR-1	16/5/01	8:00	39.34	12.593	6.6	37.8	20.3	Aerosol	0.1	0.1	4.8	115.3	0.3	3.1	1.9	5.6	7.2												
								D-SML	59.9	149.7	4.3	4.4	74.8	3.8	293.4	32.2	6.7	4.84	1.33	3.46	16.18	5.90	3.95	6.86	20.59	641.67	3.55		
								T-SML	59.1	145.3	11.7	55.2	119.1	3.8	488.3	24.6	7.6	4.89	1.43	3.46	12.88	6.26	4.37	13.75	37.82	209.75	0.68	1.518	0.063
								SSW	75.1	13.3	1.7	2.1	122.9	3.2	90.1	19.4	1.0												
TYR-2	18/5/17	8:00	39.3398	12.593	4.9	37.7	21.1	Aerosol	0.1	0.1	2.3	162.3	0.1	2.0	3.9	3.9	8.6												
								D-SML	65.7	143.6	7.9	1.1	137.7	3.9	316.3	29.8	7.7	5.53	2.00	3.57	34.60	7.08	7.58	17.87	82.21	1930.04	15.10		
								T-SML	79.9	160.6	5.3	82.5	124.9	3.6	435.2	24.4	7.9	5.00	1.87	3.16	17.26	6.61	8.15	14.30	92.93	178.71	1.84	1.725	0.071
								SSW	74.5	14.1	2.0	2.1	130.0	3.2	90.7	18.6	1.0												
St. 6	22/5/17	6:00	38.8077	14.5	10.1	37.4	20.4	Aerosol	0.1	0.1	4.8	189.8	1.2	2.2	2.7	2.9	11.3												
								D-SML	55.5	169.7	2.7	13.7	131.7	3.7	281.7	25.2	4.2	5.19	2.17	3.04	20.61	9.84	3.53	3.60	0.00	756.58	8.44		n.m
								T-SML	56.8	144.2	4.4	42.0	116.6	3.5	572.2	23.2	9.2	4.99	2.03	3.00	12.78	7.83	4.15	3.61	0.00	111.92	7.47	1.620	n.m
								SSW	72.9	15.7	1.7	2.3	131.2	3.1	86.1	18.4	1.0												
SAV	23/5/17	10:00	37.8401	17.602	3.0	38.5	20.1	Aerosol	0.1	0.1	2.1	89.9	2.1	7.1	1.4	18.5	4.9												
								D-SML	77.5	158.9	2.9	2.2	129.8	4.7	258.1	25.9	6.6	3.66	1.37	2.30	13.76	5.01	3.82	14.41	18.01	497.18	19.10	n.m	n.m
								T-SML	67.4	171.4	5.0	26.7	132.3	4.9	1028.8	27.1	7.9	3.53	1.30	2.25	12.83	6.23	5.73	3.60	14.41	104.48	3.34	n.m	n.m
								SSW	80.8	15.4	1.6	2.1	129.3	4.3	59.1	20.4	1.1												
St. 7	24/5/17	4:00	36.6035	18.166	4.8	38.5	20.8	Aerosol	0.0	0.1	2.5	85.6	0.1	4.2	1.3	8.7	6.9												
								D-SML	74.1	176.1	6.0	1.6	129.0	4.7	222.0	24.8	9.7	3.08	1.28	1.81	20.38	5.79	3.76	6.89	172.28	940.67	8.36	n.m	n.m
								T-SML	94.1	187.6	8.3	48.6	121.4	4.6	392.3	25.2	10.7	3.16	1.32	1.85	15.63	4.44	4.93	3.45	379.02	279.10	2.96	0.873	0.056
								SSW	74.0	15.8	1.7	2.9	126.2	3.9	60.1	19.7	1.0												
ION-1	25/5/17	8:00	35.4892	19.776	8.1	38.8	21.0	Aerosol	0.2	0.1	1.2	88.8	0.2	7.1	1.8	17.9	11.0												
								D-SML	53.4	188.8	3.3	5.4	91.7	5.1	284.6	38.2	9.9	2.11	0.81	1.30	17.08	5.34	3.03	13.78	68.91	823.51	26.55		n.m
								T-SML	69.8	151.5	6.8	24.7	108.4	4.6	527.9	23.9	9.1	2.19	0.88	1.32	14.29	4.71	5.88	6.88	151.29	247.57	8.20	1.790	n.m
								SSW	93.6	17.1	1.9	2.0	128.5	4.1	61.4	18.7	1.2												
ION-2	27/5/17	8:00	35.4892	19.777	12.4	38.8	21.1	Aerosol	0.0	0.0	2.9	80.6	0.1	1.7	2.5	3.8	11.3												
								D-SML	13.1	154.9	2.8	4.1	130.4	4.4	74.8	19.0	7.1	2.04	0.94	1.10	19.14	4.02	5.33	6.88	189.12	818.36	13.27		
								T-SML	13.7	168.1	5.9	30.7	127.1	4.7	74.8	28.3	13.6	2.16	0.96	1.21	9.50	0.00	4.00	0.00	275.65	310.11	7.16	1.745	0.063
								SSW	85.2	16.7	2.3	2.1	128.9	4.0	61.9	22.4	1.1												
St. 8	30/5/17	5:00	36.2103	16.631	3.7	37.9	21.2	Aerosol	0.0	0.1	2.4	89.8	0.5	4.4	1.1	11.2	12.5												
								D-SML	62.9	171.5	4.4	0.2	137.5	4.3	301.1	15.5	4.8	3.70	1.62	2.10	30.59	6.22	5.95	58.45	130.66	1688.30	26.13		
								T-SML	69.6	163.1	3.5	13.9	124.8	3.8	404.0	29.4	4.1	3.24	1.48	1.77	11.64	4.95	4.09	3.44	120.35	171.93	4.65	1.604	0.070
								SSW	76.7	16.5	1.5	3.3	123.8	3.5	62.8	16.3	1.1												
St. 9	31/5/17	16:00	38.1347	5.8408	6.2	37.1	22.0	Aerosol	0.1	0.1	1.8	170.7	0.2	2.9	5.7	4.1	10.2												
								D-SML	51.0	145.9	5.4	0.9	135.2	3.9	373.6	22.5	21.1	5.88	3.01	2.91	33.82	9.32	11.76	30.95	30.95	1248.18	37.07		
								T-SML	60.7	149.9	7.9	82.5	120.8	3.6	596.5	21.9	11.6	5.65	3.18	2.51	16.70	8.56	7.29	0.00	34.39	85.96	10.57	2.570	0.072
								SSW	66.9	14.5	1.2	2.0	130.5	3.0	91.8	21.2	1.0												
FAST-1	2/6/17	17:00	37.946	2.902	13.8	36.7	21.7	Aerosol	0.0	0.1	1.8	226.9	0.5	5.5	7.0	4.7	14.6												
								D-SML	46.6	118.5	3.8	0.1	125.4	3.4	359.1	24.0	11.9	6.20	3.55	2.68	17.11	9.54	5.07	0.00	3.45	282.54	6.93		
								T-SML	45.0	408.4	17.2	207.4	124.7	4.4	880.5	26.0	19.6	6.09	3.76	2.38	14.53	9.06	4.93	0.00	3.45	86.14	1.27	2.612	0.070
								SSW	57.3	12.0	1.1	2.8	114.3	2.5	74.4	17.5	0.7												
FAST-3	4/6/17	6:00	37.947	2.91153	4.9	36.7	21.7	Aerosol	0.1	0.2	0.9	245.3	0.2	4.5	3.4	10.2	6.8												
								D-SML	47.7	142.8	5.2	4.3	124.2	3.2	454.6	25.4	8.9	9.99	5.42	4.59	44.31	23.14	7.01	6.88	6.88	1437.29	37.29		
								T-SML	58.5	773.6	20.1	1433.3	101.9	4.5	1294.7	26.1	12.1	6.35	3.77	2.62	18.35	12.62	4.71	0.00	17.19	120.35	2.16	2.378	0.085
								SSW	57.0	12.5	1.5	1.6	120.5	2.6	74.7	19.6	1.1												
FAST-4	5/6/17	8:00	37.9467	2.91168	8.7	36.6	21.8	Aerosol	0.2	0.3	1.2	266.0	0.3	6.8	4.3	17.1	8.3												
								D-SML	53.6	115.9	4.5	3.4	125.4	2.9	247.3	17.5	4.3	8.80	4.01	4.83	44.89	18.68	7.54	10.61	799.51	1093.13	n.m		
								T-SML	57.5	96.8	17.0	64.1	116.9	3.2	635.4	20.5	20.5	6.87	3.41	3.49	43.40	12.74	7.11	3.54	2186.27	201.65	n.m	2.778	0.081
								SSW	64.4	11.9	0.8	4.0	113.0	2.5	73.2	18.4	0.6												
FAST-5	7/6/01	5:30	37.9465	2.9167	18.2	36.6	21.9	Aerosol	0.0	0.1	0.7	44.9	0.2	1.6	3.2	4.0	2.0												
								D-SML	45.0	122.7	4.6	0.0	130.3	2.9	283.3	18.9	8.3	6.61	3.22	3.41	25.04	13.76	4.39	7.08	113.20	604.94	3.14		
								T-SML	53.3	122.7	13.6	31.1	127.3	3.4	426.1	28.6	17.8	6.64	3.57	3.10	23.54	14.05	5.68	3.53	201.23	211.82	2.88	1.993	0.078
								SSW	75.5	11.9	1.3	1.8	110.8	2.5	70.9	15.4	0.9												

Table 2. Spearman's rank correlation coefficients for selected parameters. Significant correlations at $p<0.05$ and $p<0.01$ are marked with one asterisk (orange numbers) and two asterisks (red numbers), respectively.

	Variable	Latitude	Longitude	Salinity	Wind Speed	T-SML Cd	Co	Cu	Fe	Mo	Ni	Pb	V	Zn	D-SML Cd	Co	Cu	Fe	Mo	Ni	Pb	V	Zn
	Latitude	1	-0.393	-0.286	0.195	-0.319	-.575*	-0.005	0.171	0.278	-0.307	.884**	0.228	0.007	0.318	-0.405	0.373	0.212	-0.005	-0.335	0.394	-0.059	-0.126
	Longitude	-0.393	1	.883**	-0.331	.723**	.857**	.660**	0.002	0.446	.883**	-0.435	0.231	0.446	0.349	.802**	-0.315	0.311	0.11	.806**	-.535*	0.325	-0.27
	Salinity	-0.286	.883**	1	-.2	.796**	.672**	.568*	0.007	.507*	.970**	-0.298	0.459	-.682**	0.445	.620**	-0.209	0.369	-0.006	.934**	-0.432	0.304	-0.145
D-SSW	Cd	-0.319	.723**	.796**	0.032	0.232	-0.25	-.682**	-.715**	0.347	.670**	-0.435	0.194	-0.494	0.229	0.429	-0.265	0.226	0.124	.721**	-0.491	0.185	-0.3
	Co	-.575*	.857**	.672**	-0.427	0.186	0.338	-0.426	-.630**	0.054	0.39	-.495*	0.228	-0.478	0.086	.870**	-0.346	0.103	0.196	.685**	-0.301	0.277	0.015
	Cu	-0.005	.660**	.568*	0.002	0.152	0.164	-0.35	-0.414	0.093	0.314	-0.287	0.206	-0.368	0.181	0.343	-0.181	0.294	-0.201	0.38	-0.255	0.395	-0.069
	Fe	0.171	0.002	0.007	0.012	0.226	-0.072	-0.184	0.058	-0.08	-0.048	0.128	-0.318	0.055	0.387	-0.112	0.372	0.067	0.088	-0.006	0.135	-0.105	-0.105
	Mo	0.278	0.446	.507*	0.036	0.348	0.157	-.728**	-0.069	0.086	0.162	-0.002	-0.179	-0.419	0.412	0.277	-0.147	0.282	0.257	.483*	-0.191	0.27	-0.164
	Ni	-0.307	.883**	.970**	-0.341	.486*	-0.145	-.661**	-.532*	0.163	.634**	-0.327	0.086	-.699**	.487*	.630**	-0.178	0.303	0.074	.912**	-0.396	0.352	-0.14
	Pb	.884**	-0.435	-0.298	0.364	0.096	-0.365	-0.137	.547*	-0.125	-0.424	0.306	-0.287	0.017	0.115	-.485*	0.275	0.056	-0.029	-0.349	0.407	-0.064	0.012
	V	0.228	0.231	0.459	-0.153	0.359	0.058	-0.221	0.234	0.015	.525*	0.197	-0.248	-0.094	0.262	0.173	0.208	.511*	0.093	.518*	0.047	-0.043	0.131
	Zn	0.007	0.446	-.682**	-0.026	0.469	-0.034	-.677**	-0.24	0.139	0.395	-0.098	0.107	-.580*	0.404	0.152	-0.093	0.148	0.044	.621**	-0.24	0.425	-0.137
Residence Time	Cd	0.018	0.37	0.301	-.757**	.816**	0.218	-0.127	-0.088	-0.113	0.162	-0.056	-0.167	-.542*	.605*	.532*	.490*	0.13	0.103	0.432	0.23	0.081	0.132
	Co	-0.328	0.055	0.021	-.674**	0.136	.901**	0.359	0.161	-0.061	0.463	0.188	0.227	-0.113	0.064	0.289	0.144	-0.128	-0.082	0.107	0.358	0.13	0.429
	Cu	-0.108	-0.435	-.558*	-0.206	-0.262	0.282	.934**	0.338	-0.382	-0.113	0.203	-0.108	0.417	-0.373	-0.213	0.255	-0.083	-0.436	-.536*	0.319	-0.034	0.419
	Fe	0.448	-.549*	-0.462	-0.179	0.047	0.209	.510*	.926**	-0.38	-0.102	.492*	-.502*	0.258	-0.069	-0.356	0.458	0.129	-0.018	-0.407	.538*	-0.011	0.322
	Mo	-0.105	0.427	0.226	-.847**	0.468	0.328	-0.091	-0.255	0.179	0.127	-0.083	0.11	-0.431	0.456	.527*	0.201	0.005	0.221	0.318	0.118	0.007	-0.076
	Ni	-0.332	0.455	0.443	-.764**	.490*	.542*	0.054	-0.211	-0.137	.613**	0.115	0.029	-0.385	0.368	.527*	0.221	0.284	-0.164	.508*	0.137	0.118	0.24
	Pb	0.28	-.546*	-0.415	-0.056	-0.078	0.221	0.299	0.426	-0.181	0.14	.975**	-0.154	0.255	0.044	-0.4	0.093	0.15	-0.299	-0.347	.561*	-0.13	0.225
	V	-0.257	0.386	0.221	-.798**	0.309	.537*	-0.011	-0.371	0.115	0.277	-0.039	0.415	-0.409	0.336	.490*	0.08	-0.005	-0.006	0.262	0.13	0.013	-0.042
	Zn	-0.195	-0.424	-.547*	-0.004	-0.284	0.262	.826**	0.297	-0.159	-0.012	0.25	-0.11	.755**	-0.466	-0.255	0.299	-0.083	-0.194	-0.448	0.289	-0.338	0.473

Table 3. Residence times (hours) of particulate metals derived for aerosols deposition

Satation1	Co	Cu	Fe	Ni	Pb	V	Zn
St. 1	0.02	0.8	0.09	0.7	1.6	1.0	1.5
St. 3	0.05	2.8	0.13	1.0	2.0	1.9	2.7
St. 4	0.06	4.7	0.06	1.1	2.0	2.1	2.7
St. 5	0.03	1.1	0.04	0.6	1.3	1.4	1.4
TYR-1	0.05	4.4	0.10	1.0	1.1	1.9	1.6
TYR-2	0.05	2.0	0.15	0.9	1.0	1.9	1.7
St. 6	0.03	1.2	0.06	0.7	1.3	1.3	1.5
SAV	0.06	1.9	0.05	1.3	2.4	2.1	1.7
St. 7	0.06	3.1	0.09	1.2	0.9	1.9	2.3
ION-1	0.05	2.6	0.04	1.2	1.2	1.8	2.0
ION-2	0.04	1.7	0.04	0.9	0.2	1.6	2.2
St. 8	0.05	1.3	0.02	1.0	0.9	2.2	0.9
St. 9	0.04	2.2	0.11	0.7	1.4	1.2	1.9
FAST-1	0.08	3.9	0.22	0.7	2.0	1.2	2.6
FAST-3	0.25	7.6	2.53	1.2	3.0	2.0	2.6
FAST-4	0.03	6.4	0.11	0.8	1.5	1.6	4.4
FAST-5	0.02	3.1	0.03	0.5	1.0	1.3	2.3
Avergae	0.06	3.00	0.23	0.92	1.45	1.68	2.11
S.D.	0.05	1.89	0.59	0.23	0.66	0.37	0.79

Table 4. Spearman's rank correlation coefficients for selected parameters. HNA: High nucleid acid-content bacteria;: HNA; LNA: Low nucleid acid-content bacteria; CBL-small: Small cyanobacteria like cells; CBL-middle-large: middle-high cyanobacteria like cells. Significant correlations at p<0.05 and p<0.01 are marked with one asterisk (orange numbers) and two asterisks (red numbers), respectively.

	Variable	SML Bacteria	SML HNA	SML LNA	SML Pico-Phyt	SML Phyto Small	SML Phyto Middle	SML Phyto Large	SML CBL Small	SML CBL Middle-Large	SML TEP	SSW Bacteria	SSW HNA	SSW LNA	SSW Pico-Phyt	SSW Phyto Small	SSW Phyto Middle	SSW Phyto Large	SSW CBL Small	SSW CBL Middle-Large	SSW TEP	SSW PPT	SSW Chla
	Longitude	-.815**	-.842**	-.619**	-.485*	-.812**	-0.462	0.292	0.209	-0.034	0.249	-.785**	-.831**	-.516*	-.667**	-.845**	-0.329	0.321	0.166	0.433	0.416	-.630**	-.585**
	Temperature	0.427	0.377	0.265	0.191	0.184	0.255	.548*	0.187	0.233	0.377	0.341	0.394	0.011	-0.012	0.045	-0.158	-0.141	0.141	0.029	0.144	0.42	-0.132
	Salinity	-.958**	-.927**	-.797**	-0.453	-.898**	-0.338	0.159	0.28	-0.068	0.238	-.957**	-.927**	-.713**	-.565*	-.861**	-0.207	0.3	0.262	0.374	0.422	-0.412	-0.475
	Wind Speed	0.049	0.183	-0.109	0.031	0.201	-0.074	-.568*	0.027	-0.454	-.578*	0.054	0.114	-0.054	0.232	0.275	0.079	-0.047	0.187	0.087	0.078	.521*	0.187
T-SML	Cd	-0.407	-0.43	-0.238	0.161	-0.297	0.091	0.245	0.24	0.436	0.203	-0.377	-0.439	-0.11	0.186	-0.24	0.472	0.33	0.265	0.074	0.044	-0.315	0.024
T-SML	Co	-0.012	0.009	-0.174	-0.229	-0.093	-0.123	-0.127	-0.334	-0.012	0.285	-0.029	0.176	-0.245	-0.243	-0.127	-0.318	-.526*	-0.427	-0.179	-0.326	-0.265	-0.222
T-SML	Cu	.654**	.538*	.542*	0.12	.520*	0.069	-0.165	-0.118	-0.066	-0.182	.684**	.650**	0.453	0.441	.507*	0.026	-0.305	-0.077	0.066	-0.468	0.3	0.191
T-SML	Fe	.527*	.515*	.488*	.493*	.505*	.542*	-0.242	-0.181	0.267	0.024	0.449	.502*	0.449	.493*	0.456	0.33	-0.15	-0.141	-0.373	-0.421	0.424	0.371
T-SML	Ni	-.610**	-.530*	-.669**	-0.347	-.539*	-0.223	-0.15	0.063	-0.181	0.268	-.600*	-0.48	-.667**	-0.248	-0.453	-0.142	-0.183	0.001	0.15	0.15	-0.044	-0.116
T-SML	Mo	-0.238	-0.179	-0.228	-0.353	-0.287	-0.103	-0.033	0.015	-0.385	-0.344	-0.115	-0.088	-0.103	-0.186	-0.047	0	-0.234	-0.053	-0.118	-0.191	-0.206	-0.288
T-SML	Pb	0.436	-0.039	0.319	0.307	.520*	0.27	-0.371	-0.383	-0.017	0.106	0.407	0.397	0.245	0.478	.593*	0.43	-0.17	-0.444	-.578*	-0.138	.524*	.754**
T-SML	V	-0.096	-0.201	-0.201	-0.45	-0.137	-0.328	-0.114	-0.244	-0.358	-0.229	-0.066	0.135	-0.257	-0.387	-0.076	-.488*	-0.475	-0.24	-0.059	-0.265	-0.371	-0.349
T-SML	Zn	.493*	.579*	0.225	0.34	-.586*	0.257	-0.397	0.053	-0.145	-0.306	-.561*	.569*	0.245	.527*	.627**	0.166	-.554*	0.091	-0.007	-0.126	.594*	0.371
D-SML	Cd	-0.385	-0.354	-0.174	-0.085	-0.311	-0.088	0.028	0.066	0.11	-0.038	-0.338	-0.397	-0.047	-0.005	-0.25	0.266	0.348	0.043	-0.103	-0.082	-0.465	-0.108
D-SML	Co	-.583*	-.667**	-0.458	-0.444	-.544*	-.490*	0.369	-0.069	0.037	0.412	-.539*	-.559*	-0.309	-.627**	-.627**	-0.379	0.142	-0.094	0.189	0.376	-.732**	-0.495
D-SML	Cu	0.221	0.151	0.26	.712**	0.272	.645**	0.093	0.411	.652**	0.021	0.233	0.123	0.299	.738**	0.343	.619**	0.081	0.369	0.159	-0.182	0.112	.547*
D-SML	Fe	-0.301	-0.327	-0.078	0.08	-0.115	-0.069	-0.163	0.039	0.083	0.221	-0.346	-0.471	-0.044	-0.047	-0.223	-0.056	0.404	0.082	0.279	0.259	-0.029	0.279
D-SML	Ni	-.926**	-.888**	-.826**	-0.383	-.825**	-0.276	0.253	0.267	0.009	0.356	-.889**	-.853**	-.690**	-0.462	-.755**	-0.07	0.156	0.242	0.246	0.453	-0.393	-0.4
D-SML	Mo	-0.056	-0.042	-0.034	0.311	-0.074	0.431	.513*	0.219	0.407	0.359	-0.061	-0.088	0.005	-0.137	-0.103	0.048	-0.023	0.061	-0.145	0.253	-0.079	-0.002
D-SML	Pb	0.48	0.41	0.375	0.472	.512*	.495*	-0.145	-0.278	0.355	0.121	0.451	0.449	0.385	0.475	.603*	0.402	-0.221	-0.345	-0.407	-0.315	0.182	.732**
D-SML	V	-0.191	-0.265	-0.037	-.574*	-0.402	-.569*	0.146	-0.361	-0.282	0.174	-0.277	-0.208	-0.152	-0.468	-.488*	-0.219	0.366	-0.244	-0.027	-0.076	-0.182	-.670**
D-SML	Zn	0.154	0.109	-0.093	0.151	0.123	0.15	-0.08	-0.05	0.123	0.129	0.164	0.238	-0.061	0.377	0.257	0.351	-0.358	-0.064	-0.059	-0.003	0.232	0.275
D-SSW	Cd	-.826**	-.837**	-.638**	-0.421	-.809**	-0.285	0.333	0.48	-0.206	0.068	-.800**	-.882**	-.579*	-0.429	-.682**	-0.132	0.488	0.406	.512*	0.443	-0.211	-0.28
D-SSW	Co	-.586*	-.591*	-.591*	-0.418	-.608**	-0.439	0.35	-0.025	0.049	0.491	-.586*	-.532*	-.537*	-.694**	-.691**	-0.375	-0.01	-0.094	0.181	.568*	-.541*	-.538*
D-SSW	Cu	-0.412	-0.424	-0.284	-0.28	-0.434	-0.382	-0.163	-0.09	-0.069	-0.059	-0.439	-0.434	-0.252	-0.324	-0.431	-0.105	0.221	-0.055	0.326	0.126	-0.376	-0.279
D-SSW	Fe	-0.022	0.042	-0.052	0.339	0.097	0.303	-0.232	0.302	0.245	-0.235	0.036	-0.064	0.092	0.251	0.103	0.209	0.102	0.173	0.045	-0.049	-0.026	0.275
D-SSW	Ni	-.888**	-.876**	-.721**	-0.422	-.911**	-0.281	0.32	0.279	0.018	0.365	-.907**	-.899**	-.697**	-.576*	-.874**	-0.151	0.365	0.2	0.304	0.462	-0.389	-0.497
D-SSW	Mo	-0.456	-0.326	-0.429	-0.085	-0.368	-0.105	-0.018	-0.166	0.012	0.226	-.515*	-0.439	-0.326	-0.301	-0.439	0.184	0.132	-0.156	-0.292	.547*	-0.144	-0.191
D-SSW	Pb	0.306	0.348	0.321	0.389	0.373	0.392	-0.397	-0.238	0.154	-0.285	0.23	0.282	0.38	0.355	0.424	0.427	-0.005	-0.128	-0.407	-0.176	0.182	0.354
D-SSW	V	-0.467	-0.443	-0.316	0.04	-0.304	0.2	-0.058	0.139	0.096	0.258	-0.448	-0.464	-0.173	0.001	-0.216	0.177	-0.085	0.152	0.01	0.163	-0.026	0.143
D-SSW	Zn	-.602*	-.502*	-.534*	-0.113	-.599*	-0.037	0.236	0.177	0.133	0.365	-.726**	-.591*	-.664**	-0.287	-.579*	0.096	0.299	0.21	0.056	0.421	0.024	-0.251